Iranian Journal of Pharmaceutical Sciences
2023: 19 (2): 124- 138
https://journals.sbmu.ac.ir/IJPS

Original Article

Protection of Andrographolide against Paraquat-Induced Acute Lung Injury via the AMPK/Nrf2 and PI3K/Akt Pathways

Degang Zhang[a,b,c], Baohong Zhang[a,b], Yuqing Tan[a,b], Jiayi Xiao[a,b], Xuelin Ba[a], Hao Li[a], Qin Yu[a], Chenggang Zhou[d*]

[a]Lanzhou University, Lanzhou City, Gansu Province, P.R. China. [b]Lanzhou University Second Hospital, Lanzhou City, Gansu Province, P.R. China. [c]Second Clinical Medical School, Lanzhou University, Lanzhou City, Gansu Province, P.R. China. [d]The Second People's Hospital of Lanzhou City, Lanzhou City, Gansu Province, P.R. China

Abstract

Paraquat (PQ)-induced acute lung injury (ALI) remains a public concern due to its high mortality. Andrographolide (Andro) has anti-oxidative and anti-apoptosis properties. However, the role of Andro in ALI is still unknown. Herein, the purpose was to explore the function of Andro and potential mechanisms in ALI caused by PQ. An animal model of ALI was established with an intraperitoneal injection of PQ at 20mg/kg. Andro was administered intragastrically for three consecutive days. A specific AMPK inhibitor named Compd C, Nrf2 gene knockout, and a specific PI3K inhibitor named LY294002 were used to clarify the possible mechanism. Results revealed that Andro alleviated PQ-induced histopathological changes, including congestion, hemorrhage, destroyed alveoli, and extracellular matrix deposition, and inhibited apoptosis. Andro up-regulated the p-AMPK/AMPK ratio and Nrf2 and HO-1 levels while decreasing p-PI3K and p-Akt levels. In vitro, Andro appeared to reverse the PQ-induced reductions in SOD and CAT. However, Andro weakened the capacity to promote Nrf2 with Compd C and the capacity to reduce MDA and ROS while increasing SOD and CAT after the Nrf2 gene was knocked out. Additionally, Andro mitigated apoptosis by elevating the Bcl-2/Bax ratio. Results also showed that Andro promoted the Bcl-2/Bax ratio to reduce apoptosis with LY294002. In conclusion, Andro reduces the PQ-induced ALI through the AMPK/Nrf2 and PI3K/Akt pathways. The possible mechanism involves an antioxidant capacity to activate the AMPK/Nrf2 pathway and cause anti-apoptosis suppression of the PI3K/Akt pathway.

Keywords: Andrographolide; Acute lung injury; Paraquat; AMPK-activated protein kinases; Phosphatidylinositol 3-kinases; Mechanism.

Corresponding Author: Prof. Chenggang Zhou. The Second People's Hospital of Lanzhou City, Lanzhou City, Gansu Province, P.R. China.
E-mail: chenggang2025@126.com

Cite this article as: Zhang D, Zhang B, Tan Y, Xiao J, Ba X, Li H, et al, *Protection of Andrographolide against Paraquat-Induced Acute Lung Injury via the AMPK/Nrf2 and PI3K/Akt Pathways (J. Koenig ex Roxb.) Nees*, Iran. J. Pharm. Sci., 2023, 19 (2): 124- 138.

DOI: https://doi.org/ 10.22037/ijps.v19i2.43432

1. Introduction

Since 1962, paraquat (PQ) has been widely utilized in agriculture as a rapid-acting and highly toxic heterocyclic herbicide [1]. However, numerous incidences of fatal PQ poisoning occur due to both accidental and

intentional ingestion of PQ [2]. PQ is easily absorbed by other organs, particularly the lungs, due to its structural similarities to polyamines, which are prevalent in type I and II alveolar epithelial cells [3, 4]. PQ poisoning resulted in lung damage at the acute phase, presenting with clinic pathological features of congestion, alveolar hemorrhage, pneumonedema, infiltration of inflammatory cells, extracellular matrix collagen deposition, and eventually pulmonary fibrosis [5-7]. PQ mainly accumulates and destroys the structure and function of the lungs, causing progressive respiratory failure and, perhaps, death. Many research findings have verified that the inflammatory response, oxidative stress injury, and apoptosis events have significant implications for pulmonary toxicity caused by PQ [3, 8-11]. Although anti-inflammatory and anti-oxidant agents predominantly mitigate PQ intoxication, the mortality ratio remains high, to the best of our knowledge, due to a lack of specialized antidotes [12]. In order to prevent and treat PQ-induced lung toxicity, it is critically necessary to investigate alternate medications.

Andrographolide (Andro), as a kind of diterpenoid derived from the herb Andrographis paniculata, possesses some bio-activities, mainly including anti-inflammation, anti-viral, anti-oxidative, and anti-tumor properties, and has been extensively utilized as a medicinal option for treatment of the upper respiratory tract, bacillary dysentery, and gastroenteritis [13-15]. Additionally, several studies have illustrated that Andro reduces inflammation to improve ALI [16-18]. Evidence has accumulated that Andro protects against oxidative lung damage via activating Nrf2 [19, 20]. In order to maintain the balance between oxidation and antioxidants, the nuclear factor erythroid 2-related factor 2 (Nrf2) determines the synthesis of multiple kinds of antioxidant-related genes, such as heme oxygenase-1 (HO-1), superoxide dismutase (SOD), and catalase (CAT) [21-23]. Along with this, PQ-induced pulmonary toxicity is also influenced by the phosphoinositide 3-kinase (PI3K)/protein kinase B (Akt) pathway, which controls cell proliferation, growth, and metabolism [24, 25]. Additionally, accumulating evidence has verified that Andro inhibits inflammation and apoptosis via the PI3K/Akt pathway [26-28]. However, Andro's implications and possible mechanism of ALI caused by PQ are complicated and unclear. Therefore, this investigation's primary objective is to discuss Andro's biological impact on PQ-related ALI and the underlying processes related to the AMPK/Nrf2 and PI3K/Akt pathways.

2. Materials and Methods

2.1. Animals' choice

Specific pathogen-free (SPF) female C57BL/6J mice aged 4-6 weeks and weighing 18-22 g have been employed in the present research, provided to our study by the Chinese Academy of Agricultural Sciences' Lanzhou Veterinary Research Institute. All mice were maintained in sterile conditions at constant humidity levels of 50-70 % and 18-22 ℃ temperatures. Lanzhou University Second Hospital's Ethics Committee granted experiment authorization (Permit No. D2020-082).

2.2. Animal models of ALI

All mice in this experiment were allocated at random to five groups as follows: The control group, the Andro-treated along group (Sigma-Aldrich, USA), the PQ (Sigma-Aldrich, USA) group, and the low (25mg/kg)- and high (50mg/kg)-dose Andro groups [29]. To establish a model of ALI, mice in the PQ group received intraperitoneal injections of PQ with a concentration of 20mg/kg [30, 31]. An equivalent volume of saline was administered intraperitoneally to the Control mice and the Andro groups separately. Furthermore, mice received Andro at 25mg/kg and 50mg/kg intragastrically for three days after the establishment of the ALI model. Meanwhile, mice in the Control and PQ groups received intragastric saline injections of the same volume. Mice in the Andro-treated group were fed an equivalent volume of Andro at a 50mg/kg concentration.

2.3. Histopathology

The right middle lobe of the mice's lungs was extracted and preserved for 48 hours in 4% paraformaldehyde. After dehydrating the lung tissues with an alcohol concentration gradient and wax dipping, they were soaked in paraffin and sliced into five μm-thick slices. Hematoxylin-eosin (H&E) and Masson's trichrome kits (Solarbio, China) were employed to stain the slices following the manufacturer's instructions. Pathological changes were observed and photographed with an Olympus microscope after the slides were sealed with neutral gum. The lung injury was subsequently graded using the procedures previously described. In short, the pathological alterations (congestion, alveolar bleeding, wall thickening, and collagen deposition) were individually evaluated according to the following 5-level scale: No lesions or minimal, mild, moderate, serious, or highly serious lesions have been identified by 0, 1, 2, 3, and 4 scores, respectively. The mean lung damage scores in mice were used to estimate the degree of pulmonary injury.

2.4. TUNEL staining

TUNEL staining was conducted according to the manufacturer's instructions for the TUNEL kit (Servicebio, China) to analyze apoptosis in lung tissue further. The nuclei of apoptotic cells were colored red, and photographed with the IrfanView 64 program. Positive cells were counted with image analysis by randomly selecting three areas under a microscope (Olympus, Japan).

2.5. Immunohistochemistry (IHC) analysis

Immunohistochemistry (IHC) was used to assess the amounts of the anti-apoptotic protein Bcl-2 and the pro-apoptotic protein Bax in lung tissues, and the outcomes are as follows: 5μm-thick slices were roasted for 1 hour, then deparaffinized in xylene, rehydrated utilizing graded ethanol solutions, and microwaved in a sodium citrate buffer. After cooling, the slides were treated with 3% hydrogen peroxide for 1 hour before being blocked with 5% BSA at ambient temperatures. After which, slices were incubated overnight at 4℃ with anti-Bcl-2 (Proteintech, 1:500) and anti-Bax (Proteintech, 1:1,000) primary antibodies. Then, the sections were incubated for 1 hour at room temperature with a secondary antibody (Biosharp, 1:1,000)

after being rinsed three times with PBS. A DAB substrate was applied to the slices for 8 minutes. Ultimately, the slides were inspected and captured using the IrfanView 64 program.

2.6. Cell Culture

Type II mouse epithelial cells named MLE-12 cells were acquired from the American Type Culture Collection (ATCC, USA). Cells were maintained in DMEM/F-12 (1:1) (Gibco, USA) supplemented with 10% fetal bovine serum (Cell Box, China) as well as 1% antibiotics (Biosharp, China), and were then incubated at 37 ℃ in a 5% CO_2 atmosphere before being trypsinized (Gibco, USA). The CCK-8 test has previously been used to examine the effects of Andro on PQ-related cytotoxicity in MLE-12 cells [32]. In brief, MLE-12 cells were seeded onto 6-well sterile plates at a density of 1×10^5/well and cultivated for 48 hours at 37 ℃ in a 5% CO2 environment. MLE-12 cells were pretreated with Andro for 6 hours before being exposed to PQ for 24 hours, with cell density reaching 80-90% on 6-well sterile plates. Finally, MLE-12 cells were harvested for the following investigations.

2.7. Transfection

MLE-12 cells were planted in 6-well plates at a density of up to 30-40% for 24 hours before being transfected with Nfe2l2 siRNA sequences as per the instructions provided by the manufacturer (HANBIO, China). The following are the Nrf2 siRNA detail sequences: 5'-GACUCAAAUCCCACCUUAAdTdT-3' is the sense strand, while 5'-UUAAGGUGGGAUUUGAGUCdTdT-3' is the anti-sense strand. Following 48 hours of transfection, MLE-12 cells were cultured for two days with 4g/ml puromycin. Finally, the cells with Nrf2 silence were collected for the following study.

2.8. Assays for reactive oxygen species (ROS)

In vitro, ROS detection was accomplished using DCFH-DA (Biosharp, China) as a fluorescent probe. After removing the cell culture solution, 5μM DCFH-DA was added, diluted in a serum-free medium, and applied to each plate well. It was followed by 30 minutes of incubation in an incubator at 37℃. Ultimately, samples were analyzed via Beckman's CytoFLEX flow cytometry (Beckman, USA).

2.9. Apoptosis analysis

MLE-12 cell apoptosis was identified using the Annexin V-FITC/PI reagent (Biosharp, China). Cells were then trypsinized, washed, and resuspended using a staining solution before being treated for 30 minutes at room temperature with Annexin V-FITC/PI solution. At last, CytoFLEX flow cytometry (Beckman, USA) was used to guarantee an adequate cell apoptosis rate.

2.10. Oxidative stress markers

MLE-12 cells were collected and split by an ultrasonic cell fragmentation instrument (SONICS, USA) with an associated power of 300 watts. This process was repeated 5 times for 5 seconds with an interval of 30 seconds. The experiment was conducted strictly according to the instructions set by the Nanjing Jiancheng Bioengineering Institute, China. The absorption spectrum value was determined by the enzyme micro-plate reader (Thermo Fisher, USA).

2.11. Western Blot

Total proteins were collected and isolated using RIPA (Beyotime, China). Protein concentrations were determined using the BCA Protein Assay Kit (Biosharp, China). Equal protein samples were processed on 10% SDS-PAGE (Biosharp, China) to separate various proteins. After that, the proteins were transferred to a 0.22μM PVDF membrane (Millipore, USA) and blocked in 5% BSA for 1 hour (Biosharp, China). And the PVDF membrane was incubated overnight in a refrigerator at 4℃with the following antibodies: AMPK (Proteintech, 1: 1,000), p-AMPK (CST, 1: 1,000), HO-1 (Abcam, 1: 10,000), Nrf2 (Abconol, 1: 1,000), p-PI3K (CST, 1: 1,000), p-Akt (CST, 1: 1,000), Bax (Proteintech, 1: 5,000), Bcl-2 (Proteintech, 1: 1,000), and β-actin (Servicebio, 1: 2,500). After washing with TBST (Servicebio, China), the second antibody (Biosharp, 1: 10,000) was administered with membranes for an hour. The proteins were observed using the hypersensitive ECL (Biosharp, China). Finally, Image J software performed western blot quantification and scanned blot analysis.

2.12. Statistics and analysis

All values in this article were presented as means ± standard deviation (SD). The statistical analysis was carried out using the GraphPad Prism 8.0 program (GraphPad Inc., USA). A one-way analysis of variance (ANOVA) was used for contrasting various groups, followed by Turkey's multiple comparison tests. A P-value of 0.05 or 0.01 was considered statistically significant.

3. Results and Discussion

3.1. Andro attenuates the ALI caused by PQ in mice by pathological analysis

In PQ-induced ALI animal models, we observed alveolar structural integrity without congestion, bleeding, or collagen fiber deposition in the lungs of mice. It was observed using HE and Masson staining. Furthermore, there were no differences in lung injury scores between the Control and Andro-treated groups ($P>0.05$) (**Figure 1B**). However, PQ stimulation induced observable histopathological changes in the characteristics of lung congestion, hemorrhage, structural destruction of alveoli, and extracellular matrix deposition when compared to the Control group, as shown in Figures 1A and 1C ($P<0.01$) (**Figures 1A and C**). PQ poisoning has been investigated and shown to be a major contributor to pesticide death [33, 34]. It is reported that ingestion of primary paraquat was responsible for one-fifth of pesticide deaths in South Korea, and case fatalities were also high in Iran [35, 36]. Since the lungs suffered severe damage after exposure to PQ, experimental tests have also proved this conclusion. To our knowledge, no effective treatment for preventing and treating PQ poisoning has been discovered. Therefore, new medications to mitigate its toxicity are urgently needed to minimize the high mortality caused by PQ.

Andro, as a critical bioactivity ingredient extracted from the natural plant Andrographis paniculata, is well known for its potent antiviral, antioxidant, and anti-inflammatory properties, which have been widely used to treat an array of

diseases, including osteoarthritis, upper respiratory diseases, as well as multiple sclerosis [37]. Nevertheless, Andro's roles and possible mechanisms in PQ-related ALI are still complicated and unknown. Therefore, we evaluated the role of Andro against PQ-induced ALI. Interestingly, Andro at different concentrations (25 and 50 mg/kg) significantly reduced lung histological alterations and lowered the lung score and collagen deposition in animal experiments. Thus, our findings indicated that Andro substantially decreased ALI caused by PQ by reducing alveolar congestion, hemorrhage, and structural destruction and lowering extracellular matrix deposition in animal models (P<0.01) (**Figure 1**).

3.2. Andro mitigates apoptosis in the PQ-induced ALI in lungs in mice.

There is mounting evidence that apoptosis contributes to the progression of PQ-induced pulmonary toxicity [3, 38, 39]. Therefore, TUNEL labeling was used to detect the degree of apoptosis in vivo. Results illustrated that the TUNEL-positive cells of apoptosis increased significantly after PQ stimulation, compared with the Control group, and had a statistically significant difference (P<0.01) (**Figures 2A** and **2D**). B-cell lymphoma 2 (Bcl-2) is a pioneering member of the Bcl-2 family of apoptosis-regulating proteins. Bcl-2 protein effectively prevents the aggregation of pro-apoptotic proteins Bax, reduces the release of apoptosis-related factors, and plays an anti-apoptosis role [40].

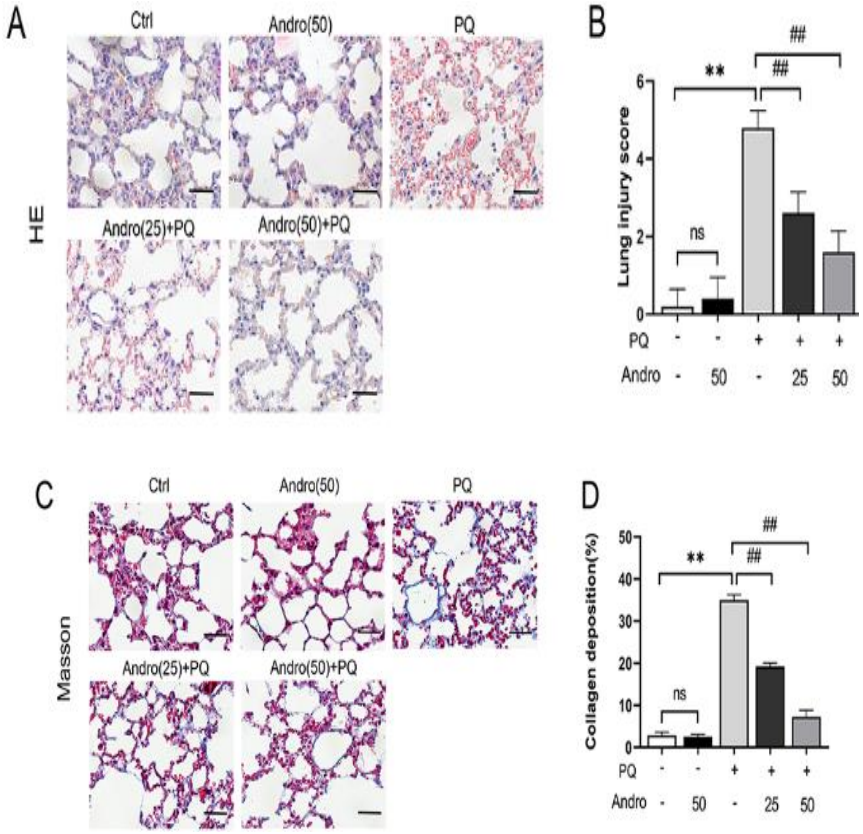

Figure 1. Andro attenuates the ALI caused by PQ in mice. **(A)** Histopathology changes by H&E staining (magnification: 200×). **(B)** Lung injury score. **(C)** Collagen deposition changes assessment by Masson trichrome staining (magnification: 200×). **(D)** Collagen deposition area ratio. Data are presented as the means ± SD. "ns" means no significant difference with the Control group; *P<0.05, **P < 0.01 vs. the Control group; $^{\#}$P<0.05, $^{\#\#}$P<0.01 vs. the PQ group.

The immunohistochemical approach in vivo was further used to investigate the probable molecular mechanisms of apoptosis by analyzing the Bcl-2 and Bax levels. In studies of PQ-related toxicity, the expression of Bax was significantly up-regulated, and the expression of Bcl-2 was significantly down-regulated, suggesting that PQ induced apoptosis events by regulating the imbalance between Bcl-2 and Bax levels. In experiments, a substantial reduction of Bcl-2 expression and a significant rise in Bax expression in lung tissues were observed compared with the Control group (P<0.01) (**Figures 2B, 2C, 2E, and 2F**). PQ induces apoptosis by causing an imbalance between anti-apoptotic and pro-apoptotic proteins, consistent with previous studies [38, 39]. However, Andro treatments with concentration effects substantially lowered the amount of TUNEL-positive cells in contrast to the PQ group (P<0.01) (**Figures 2A and 2D**). Moreover, we did detect a difference between the Bcl-2 and Bax protein levels in the PQ and Andro-treated groups with different doses (25 mg/kg and 50mg/kg, separately); Andro treatments, on the other hand, completely reversed the PQ-induced fail in Bcl-2 as well as the rise in Bax expression (P<0.01) (**Figures 2B, 2C, 2E, and 2F**). These findings demonstrate that Andro mitigates PQ-induced apoptosis by modulating Bcl-2 and Bax expression.

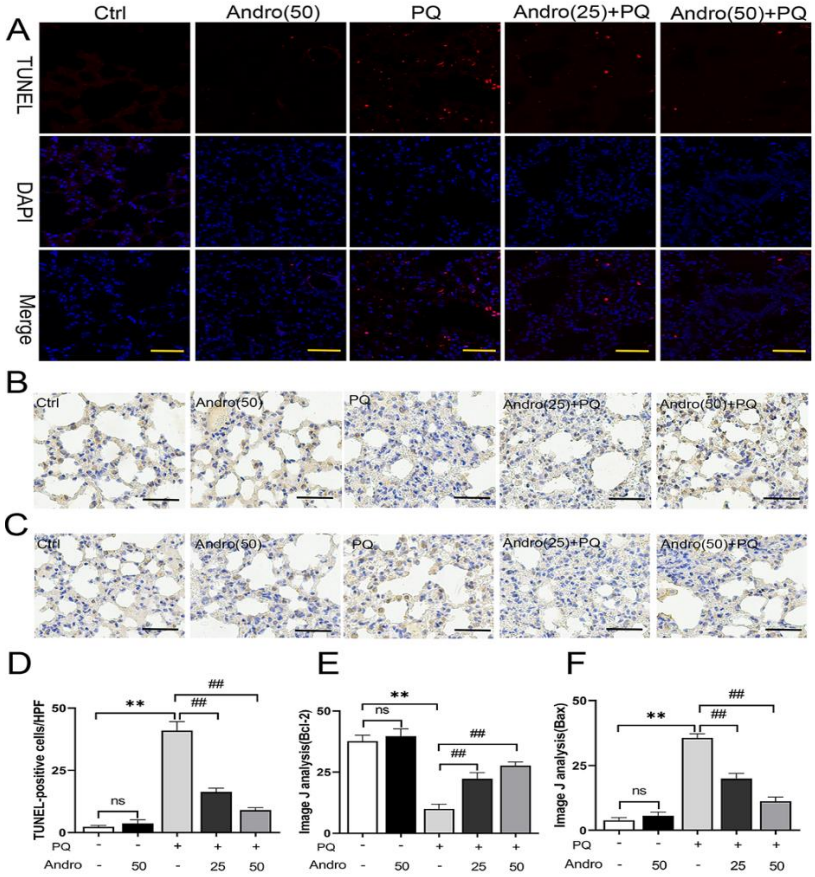

Figure 2. Andro mitigates apoptosis in the PQ-induced ALI in the lungs of mice. **(A)** Detection of apoptosis (magnification: 200×). The levels of **(B)** anti-apoptosis protein Bcl-2 and **(C)** pro-apoptosis protein Bax were tested by IHC (magnification: 200×). **(D)** Quantitative analysis of apoptosis in the lungs. Expression levels of **(E)** Bcl-2 and **(F)** Bax were analyzed by Image J. The results are expressed as mean ± SD. "ns" means no significant difference with the Control group; $^{*}P < 0.05$, $^{**}P < 0.01$ vs. the Control group; $^{\#}P < 0.05$, $^{\#\#}P < 0.01$ vs. the PQ group.

3.3. Andro regulates the AMPK/Nrf2 and PI3K/Akt pathways in PQ-induced ALI in mice.

The AMP-activated protein kinase (AMPK)/ factor-erythroid 2 related factor 2 (Nrf2) plays critical roles in oxidative stress-associated diseases [41, 42]. Thus, Western blotting in mice's lungs explored the AMPK/Nrf2 signaling pathways. Our findings confirmed that the p-AMPK/AMPK ratio and the expression of the antioxidant protein Nrf2 were considerably elevated following the PQ stimulation. PQ raised HO-1 in the lungs; it is the primary antioxidant protein downstream of Nrf2 (P<0.01) (**Figure 3A-D**). Nrf2, as an important antioxidant key factor, effectively activates the essential downstream protein Heme Oxygenase-1 (HO-1) and controls the synthesis of antioxidant enzyme genes when subjected to oxidative stress injury [43, 44]. Hence, this phenomenon- the increase of p-AMPK, Nrf2, and HO-1 expression is closely associated with initiating the anti-oxidative defense mechanism in mice after exposure to PQ. Moreover, western blotting results also illustrated that the p-AMPK/AMPK ratio, as well as the antioxidant proteins, Nrf2 and HO-1 levels, were significantly up-regulated following Andro with varied dosage treatments when compared to the PQ group (P<0.01) (**Figure 3A-D**). These demonstrated that Andro strengthens mice's antioxidant capacity by stimulating the AMPK/Nrf2 pathway to attenuate the PQ-induced ALI.

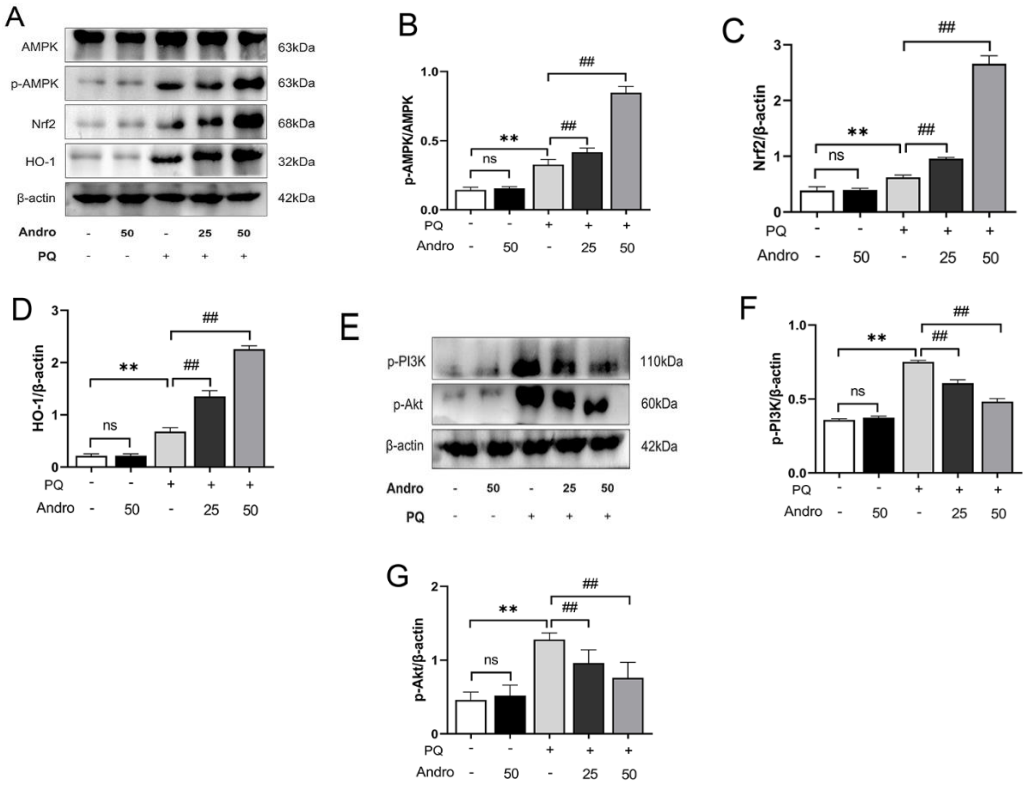

Figure 3. Andro regulates the AMPK/Nrf2 and PI3K/Akt pathways in PQ-induced ALI. **(A)** Western blot analysis was performed to detect the expression of AMPK, p-AMPK, Nrf2, and HO-1 in the lungs of mice. Representative Western blot images and quantitative analysis of **(B)** the ratio of p-AMPK and AMPK, **(C)** Nrf2, and **(D)** HO-1. **(E)** Western blot analysis was performed to detect the expression of p-PI3K and p-Akt in mice. Representative Western blot images and quantitative analysis of **(F)** p-PI3K and **(G)** p-Akt. The results are expressed as mean ± SD. "ns" means no significant difference with the Control group; *P<0.05, **P<0.01 vs. the Control group; $^{\#}$P<0.05, $^{\#\#}$P<0.01 vs. the PQ group.

In addition, the possible role of the PI3K/Akt pathway was also investigated. There was no difference in p-PI3K and p-Akt protein levels between the Control and Andro-treated groups. In contrast to the Control group, PQ-induced ALI raised p-PI3K and p-Akt levels, whereas Andro treatment dramatically decreased the p-PI3K and p-Akt expression levels compared with the PQ group in a dose-dependent manner ($P<0.01$) (**Figure 3E-G**). To summarize, Andro protected mice against PQ-related ALI in mice via inhibiting the PI3K/Akt pathway.

3.4. Andro activates the AMPK/Nrf2 pathway to relieve oxidative stress in MLE-12 cells.

Accumulating research findings support that oxidative stress is closely associated with PQ-induced poisoning [11, 24, 45]. The oxidation and antioxidant mechanisms imbalance results in oxidative stress [46]. The initial explanation for oxidant stress in PQ-associated pulmonary toxicity is reactive oxygen species (ROS). Excessive ROS causes lipid peroxidation as well as the formation of reactive aldehyde byproducts like malondialdehyde (MDA), and degrades cell function by triggering apoptosis and inflammatory responses following PQ exposure [47]. Hence, the oxidative stress induced by PQ and the effect of Andro were further investigated in vitro. When the PQ concentration was 950.2μM, MLE-12 cell viability was markedly inhibited by half, and Andro's concentration was 25μM: its capacity to minimize PQ cytotoxicity was optimal in our previous studies [32]. Thus, the concentration of 25μM Andro and PQ at 950.2μM was chosen as the optimum dose for this study. Results showed that PQ induced MLE-12 cells to generate large amounts of ROS and MDA compared to the Control group ($P < 0.05$) (**Figure 4A-C**).

Superoxide dismutase (SOD) and catalase (CAT), as the primary antioxidant capacity administrators, reduce oxidative damage caused by ROS and MDA in order to maintain the balance between oxidation and antioxidants under physiological conditions [48]. When the generation of ROS and MDA surpasses the antioxidant capacity, oxidative stress damage ensues. Following PQ with a 950.2μM stimulus for 24 h, the antioxidant enzyme expression levels of SOD and CAT declined dramatically, while the generation of ROS and MDA was considerably raised in MLE-12 cells ($P<0.05$) (**Figure 4A-C**). Hence, our findings further confirmed that oxidative stress is associated with the incidence of PQ-induced ALI, consistent with the previous studies [4, 11]. Nevertheless, in comparison to the PQ group, Andro substantially increased SOD and CAT levels while decreasing ROS and MDA, which reveals the antioxidant capacity of Andro against the PQ-associated oxidant stress injury ($P<0.05$) (**Figure 4A-C**).

Moreover, results illustrated that PQ induced the activation of the AMPK/Nrf2 pathway in MLE-12 cells by raising the p-AMPK/AMPK ratio, Nrf2, and HO-1 levels, and Andro enhanced a more significant increase in the p-AMPK/AMPK ratio, Nrf2, and HO-1 levels when compared to the PQ group. A specific AMPK inhibitor named Compd C was further employed to explore its function of the AMPK/Nrf2 pathway in Andro's alleviation of the PQ-related cytotoxicity. Results displayed that Andro's ability to increase the expression of Nrf2, a key antioxidant protein, was weakened after inhibiting the expression of p-AMPK in cells. Our findings in vitro mean that Andro activates the AMPK/Nrf2 pathway to relieve the PQ-related cytotoxicity ($P<0.01$) (**Figure 4F-H**).

In addition, we further assumed that PQ might initially activate the AMPK/Nrf2 pathway to increase SOD and CAT production, therefore initiating anti-oxidative defense to lower oxidative stress in vitro. Therefore, in follow-up experiments, we investigated the critical role of Nrf2 in the protective role of Andro since Nrf2 plays an essential role in antioxidant enzyme expression, including SOD and CAT. Following Andro treatment, the levels of p-AMPK, Nrf2, and HO-1 were significantly increased, reducing PQ-induced overproduction of ROS and MDA. Andro treatment with the forced knockout of the Nrf2 gene did not reverse the reduction in SOD and CAT, nor did it affect the rise in ROS and MDA caused by PQ ($P<0.05$) **(Figure 4A-E).** Lv *et al*. studied the mechanisms of LPS-induced ALI, and detected the pivotal role of AMPK/Nrf2 pathway by lessening ROS and MDA generation [49]. Huang *et al*. also emphasized the importance of AMPK/Nrf2 in LPS-induced ALI [50]. Likewise, we have also confirmed that the AMPK/Nrf2 signaling pathway is critical in PQ-induced ALI. In vitro, however, Andro did not increase antioxidant capacity or diminish PQ-induced oxidative damage in the presence of Nrf2 deletion. As a result, our findings demonstrated that PQ triggered the AMPK/Nrf2 pathway, and then Andro specifically engaged the AMPK/Nrf2 pathway to ameliorate PQ-induced oxidative stress in vitro.

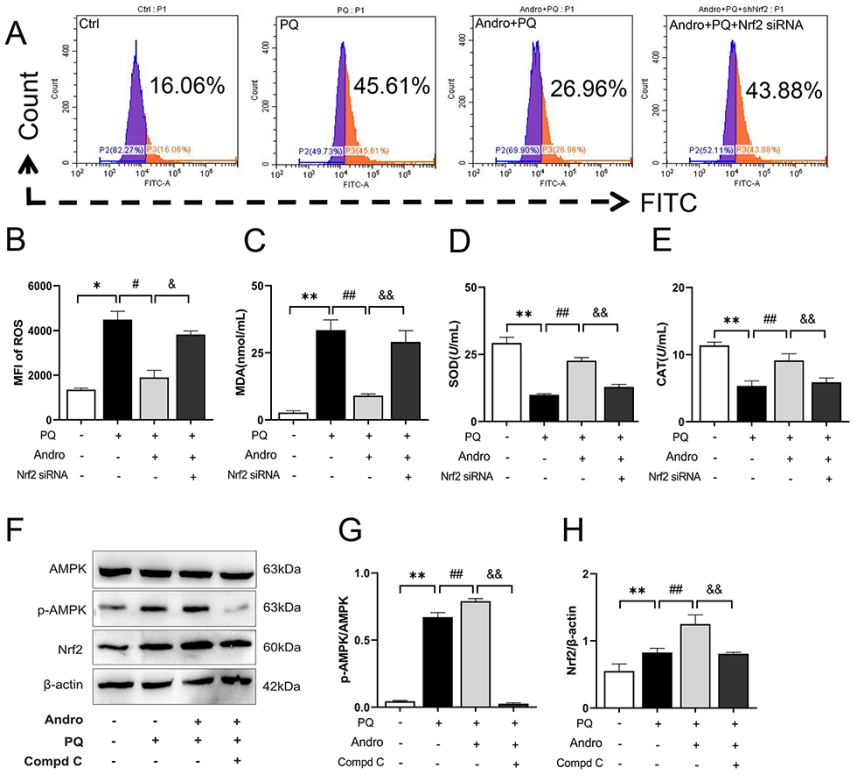

Figure 4. Andro activates the AMPK/Nrf2 pathway to relieve oxidative stress in MLE-12 cells. **(A)** The ROS level was evaluated by flow cytometry via DCFH-DA in the forced silence of Nrf2 in MLE-12 cells. **(B)** Mean fluorescence of DCF. **(C)** The assay kits in cells assessed MDA level, **(D)** SOD activity and **(E)** CAT content of oxidant stress. **(F)** Western blot was performed to detect the expression of AMPK, p-AMPK, and Nrf2 proteins in vivo with a specific AMPK inhibitor named Compd C. Representative Western blot images and quantitative analysis of **(G)** the p-AMPK/AMPK ratio and **(H)** Nrf2 proteins. Data are presented as the means ± SD. Andro was added 6 hours prior to PQ treatment for 24 hours. $^{*}P<0.05$, $^{**}P<0.01$ vs. the Control group; $^{\#}P<0.05$, $^{\#\#}P<0.01$ vs. the PQ group. $^{\&}P<0.05$, $^{\&\&}P<0.01$ vs. the Andro+ PQ group.

3.5. Andro inhibits apoptosis via the PI3K/Akt pathway in vitro

The phosphoinositide 3-kinase (PI3K)/protein kinase B (Akt) pathway regulates apoptosis, which is connected to PQ-related ailments [51, 52]. Our findings confirmed that PQ dramatically increased the levels of p-PI3K and p-Akt in vitro and in vivo, according to the previous study [53]. Nevertheless, Andro significantly abolished the increase of PQ-induced p-PI3K and p-Akt in vitro. These findings also disclose that Andro effectively suppresses the PI3K/Akt pathway to reduce PQ-related cytotoxicity at the cellular level. Besides, MLE-12 cells exhibited more apoptosis after 24 hours of PQ treatment than the Control group. However, Andro pretreatment for 6 hours significantly decreased the incidence rate of apoptosis in contrast to the PQ group. Thus, our data showed that Andro eased PQ-induced apoptosis in MLE-12 cells ($P<0.01$) (**Figures 4A and 4B**).

Hsueh *et al*. elaborated on how the PI3K/Akt pathway inhibits apoptosis during ALI [54]. However, whether Andro determines apoptosis via the PI3K/Akt pathway to lessen paraquat-mediated apoptosis is uncertain. Hence, LY294002, a specific inhibitor of PI3K, was employed to examine the potential function of the PI3K/Akt signalling pathway in Andro's inhibiting PQ-induced apoptosis in vitro. Results showed that Andro suppressed the increase of PQ-induced apoptosis with LY294002 compared with the Andro group, according to the flow cytometry analysis ($P<0.01$) (**Figures 5A and 5B**). Anti-apoptotic protein Bcl-2 and pro-apoptotic protein Bax both play significant roles in regulating the beginning and progression of apoptosis [55]. Consequently, we further discussed the Bcl-2 to Bax ratio in PQ-induced apoptosis. The ratio of Bcl-2/Bax was notably decreased in the PQ group, whereas Andro pretreatment distinctly reversed this decline. Furthermore, Andro with LY294002 significantly increased the Bcl-2/Bax ratio compared to Andro pretreatment before the PQ stimulation ($P<0.01$) (**Figures 5C and 5F**). Collectively, these data revealed that Andro promoted the ratio of Bcl-2/Bax to reduce PQ-induced apoptosis via inhibiting the PI3K/Akt signalling pathway.

4. Conclusion

In short, this research demonstrated that in vivo and in vitro, PQ-induced ALI involves oxidative stress and apoptosis. Moreover, based on the above findings, it was clear that the AMPK/Nrf2 and PI3K/Akt pathways, which control oxidative stress and apoptosis, respectively, both played significant roles in ALI caused by PQ. The underlying potential mechanism of Andro in alleviating the PQ-related ALI involved the reduction of oxidative stress by activating the AMPK/Nrf2 pathway, as well as the inhibition of apoptosis by suppressing the PI3K/Akt pathway to increase the ratio of Bcl-2 to Bax.

Acknowledgments

None.

Conflict of interest

The authors declare to have no conflict of interest.

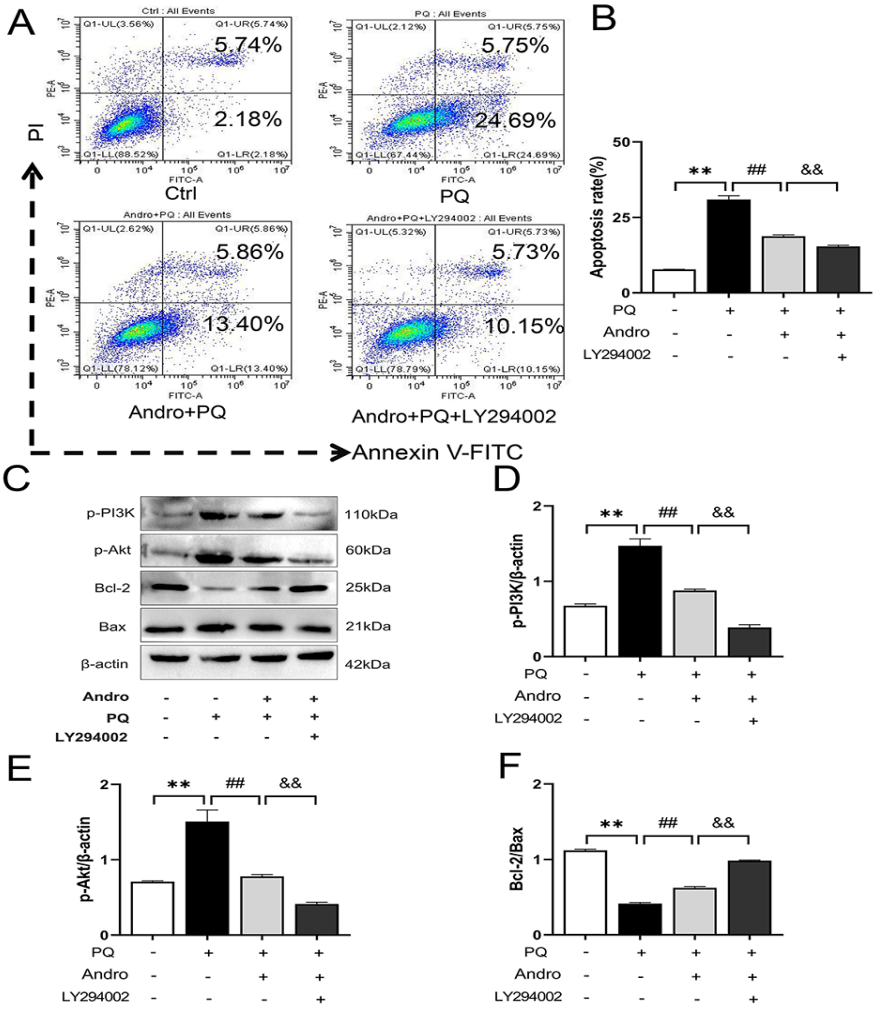

Figure 5. Andro attenuates apoptosis by inhibiting the PI3K/Akt pathway in vitro. **(A)** Andro significantly reduced apoptosis by flow cytometry analysis. (**B**) Comparisons of apoptosis ratios in MLE-12 cells. **(C)** Western blot analysis determined the protein expression of p-PI3K, p-Akt, Bcl-2, and Bax with a specific PI3K inhibitor named LY294002 in MLE-12 cells. Representative Western blot images and quantitative analysis of **(D)** p-PI3K, **(E)** p-Akt, and **(F)** the Bcl-2/Bax ratio in MLE-12 cells. Data are presented as the means ± SD. Andro was added 6 hours prior to PQ treatment for 24 hours. $^{*}P < 0.05$, $^{**}P < 0.01$ vs. the Control group; $^{\#}P < 0.05$, $^{\#\#}P < 0.01$ vs. the PQ group. $^{\&}P < 0.05$, $^{\&\&}P < 0.01$ vs. the Andro+PQ group.

Funding

This work was supported by the National Natural Science Foundation of China (grant number 82260325, 81960014); Project of Administration of Traditional Chinese Medicine of Gansu Province (grant number GZKP-2021-31); Gansu Health Industry Scientific Research Program (grant number GSWSKY2021-061); Higher Education Innovation Fund Project of Gansu Province (grant number 2021B-028); Science and Technology Planning Project of Lanzhou City (grant number 2020-XG-59); Undergraduate Innovation and Entrepreneurship Project of Lanzhou University (grant numbers 20210050067, 220210904030); Cuiying Science and Technology Innovation Project of Lanzhou University Second Hospital (grant number 2020QN-23), and Cuiying Scientific

Training Program for Undergraduates of Lanzhou University Second Hospital (grant numbers CYXZ2022-35, CYXZ2023-23).

References

[1] Eddleston M, Nagami H, Lin CY, Davis ML, Chang SS. Pesticide use, agricultural outputs, and pesticide poisoning deaths in Japan. Clin Toxicol (Phila) (2022) 60 (8): 933-941.

[2] Buckley NA, Fahim M, Raubenheimer J, Gawarammana IB, Eddleston M, Roberts MS, Dawson AH. Case fatality of agricultural pesticides after self-poisoning in Sri Lanka: a prospective cohort study. Lancet Glob Health (2021) 9 (6): e854-e862.

[3] Subbiah R, Tiwari RR. The herbicide paraquat-induced molecular mechanisms in the development of acute lung injury and lung fibrosis. Crit Rev Toxicol (2021) 51 (1): 36-64.

[4] Dinis-Oliveira RJ, Duarte JA, Sánchez-Navarro A, Remião F, Bastos ML, Carvalho F. Paraquat poisonings: mechanisms of lung toxicity, clinical features, and treatment. Crit Rev Toxicol (2008) 38 (1): 13-71.

[5] Amirshahrokhi K, Bohlooli S. Effect of methylsulfonylmethane on paraquat-induced acute lung and liver injury in mice. Inflammation (2013) 36 (5): 1111-1121.

[6] Liu Y, Li Z, Xue X, Wang Y, Zhang Y, Wang J. Apigenin reverses lung injury and immunotoxicity in paraquat-treated mice. Int Immunopharmacol (2018) 65: 531-538.

[7] Okabe R, Chen-Yoshikawa TF, Yoshizawa A, Hirashima T, Saito M, Date H, Takebe T. Orthotopic foetal lung tissue direct injection into lung showed a preventive effect against paraquat-induced acute lung injury in mice. Eur J Cardiothorac Surg (2020) 58 (3): 638-645.

[8] SreeHarsha N. Embelin impact on paraquat-induced lung injury through suppressing oxidative stress, inflammatory cascade, and MAPK/NF-κB signaling pathway. J Biochem Mol Toxicol (2020) 34 (4): e22456.

[9] Amin F, Roohbakhsh A, Memarzia A, Kazerani HR, Boskabady MH. Immediate and late systemic and lung effects of inhaled paraquat in rats. J Hazard Mater (2021) 415: 125633.

[10] Chen J, Jian X, Li C, Cheng B. Therapeutic potential of amitriptyline for paraquat-induced pulmonary fibrosis: Involvement of caveolin-1-mediated anti-epithelial-mesenchymal transition and inhibition of apoptosis. Ecotoxicol Environ Saf (2023) 254: 114732.

[11] Amin F, Memarzia A, Roohbakhsh A. Zataria multiflora and Pioglitazone Affect Systemic Inflammation and Oxidative Stress Induced by Inhaled Paraquat in Rats. Mediators Inflamm (2021) 2021: 5575059.

[12] Li LR, Chaudhary B, You C, Dennis JA, Wakeford H. Glucocorticoid with cyclophosphamide for oral paraquat poisoning. Cochrane Database Syst Rev (2021) 6 (6): Cd008084.

[13] Dai Y, Chen SR, Chai L, Zhao J, Wang Y, Wang Y. Overview of pharmacological activities of Andrographis paniculata and its major compound andrographolide. Crit Rev Food Sci Nutr (2019) 59(sup 1): s17-s29.

[14] Kumar G, Singh D, Tali JA, Dheer D, Shankar R. Andrographolide: Chemical modification and its effect on biological activities. Bioorg Chem (2020) 95:103511.

[15] Enmozhi SK, Raja K, Sebastine I, Joseph J. Andrographolide as a potential inhibitor of SARS-CoV-2 main protease: an in silico approach. J Biomol Struct Dyn (2021) 39 (9): 3092-3098.

[16] Gao J, Peng S, Shan X, Deng G, Shen L, Sun J, Jiang C, et al. Inhibition of AIM2 inflammasome-mediated pyroptosis by Andrographolide contributes to amelioration of radiation-induced lung inflammation and fibrosis. Cell Death Dis (2019)10 (12): 957.

[17] Peng S, Hang N, Liu W, Guo W, Jiang C, Yang X, Xu Q, et al. Andrographolide sulfonate ameliorates lipopolysaccharide-induced acute lung injury in mice by down-regulating MAPK and NF-κB pathways. Acta Pharm Sin B (2016) 6 (3): 205-211.

[18] Li T, Zhang C, Wei Y, Zhong H, Shan L, Yu P, Wang Y, et al. Andrographolide Derivative AL-1

Ameliorates LPS-induced Acute Lung Injury by Inhibiting NLRP3 Inflammasome and Lung Permeability. Curr Pharm Des (2022) 28 (30): 2508-2517.

[19] Mussard E, Cesaro A, Lespessailles E, Legrain B, Berteina-Raboin S, Toumi H. Andrographolide, a Natural Antioxidant: An Update. Antioxidants (Basel) (2019) 8 (12): 571.

[20] Liao W, Lim AYH, Tan WSD, Abisheganaden J, Wong WSF. Restoration of HDAC2 and Nrf2 by andrographolide overcomes corticosteroid resistance in chronic obstructive pulmonary disease. Br J Pharmacol (2020) 177 (16): 3662-3673.

[21] Ma Q. Role of nrf2 in oxidative stress and toxicity. Annu Rev Pharmacol Toxicol (2013) 53: 401-426.

[22] Thiruvengadam M, Venkidasamy B, Subramanian U, Samynathan R, Ali Shariati M, Rebezov M, Girish S, et al. Bioactive Compounds in Oxidative Stress-Mediated Diseases: Targeting the NRF2/ARE Signaling Pathway and Epigenetic Regulation. Antioxidants (Basel, Switzerland) (2021) 10 (12): 1859.

[23] Zhang Q, Liu J, Duan H, Li R, Peng W, Wu C. Activation of Nrf2/HO-1 signaling: An important molecular mechanism of herbal medicine in the treatment of atherosclerosis via the protection of vascular endothelial cells from oxidative stress. J Adv Res (2021) 34: 43-63.

[24] Liu X, Yang H, Liu Z. Signaling pathways involved in paraquat-induced pulmonary toxicity: Molecular mechanisms and potential therapeutic drugs. Int Immunopharmacol (2022) 113(Pt A): 109301.

[25] Alzahrani AS. PI3K/Akt/mTOR inhibitors in cancer: At the bench and bedside. Semin Cancer Biol (2019) 59: 125-132.

[26] Duan MX, Zhou H, Wu QQ, Liu C, Xiao Y, Deng W, Tang QZ. Andrographolide Protects against HG-Induced Inflammation, Apoptosis, Migration, and Impairment of Angiogenesis via PI3K/AKT-eNOS Signalling in HUVECs. Mediators Inflamm (2019) 2019: 6168340.

[27] Bodiga VL, Bathula J, Kudle MR, Vemuri PK, Bodiga S. Andrographolide suppresses cisplatin-induced endothelial hyperpermeability through activation of PI3K/Akt and eNOS -derived nitric oxide. Bioorg Med Chem (2020) 28 (23): 115809.

[28] Tohkayomatee R, Reabroi S, Tungmunnithum D, Parichatikanond W, Pinthong D. Andrographolide Exhibits Anticancer Activity against Breast Cancer Cells (MCF-7 and MDA-MB-231 Cells) through Suppressing Cell Proliferation and Inducing Cell Apoptosis via Inactivation of ER-α Receptor and PI3K/AKT/mTOR Signaling. Molecules (Basel, Switzerland) (2022) 27 (11): 3544.

[29] Gao F, Liu X, Shen Z, Jia X, He H, Gao J, Wu J,et al. Andrographolide Sulfonate Attenuates Acute Lung Injury by Reducing Expression of Myeloperoxidase and Neutrophil-Derived Proteases in Mice. Front Physiol. (2018) 9: 939.

[30] He Q, Zhang W, Zhang J, Deng Y. Cannabinoid Analogue WIN 55212-2 Protects Paraquat-Induced Lung Injury and Enhances Macrophage M2 Polarization. Inflammation (2022) 45(6): 2256-2267.

[31] Amirshahrokhi K, Khalili AR. Carvedilol attenuates paraquat-induced lung injury by inhibition of proinflammatory cytokines, chemokine MCP-1, NF-κB activation and oxidative stress mediators. Cytokine (2016) 88:144-153.

[32] Zhang D, Shen F, Ma S, Nan S, Ma Y, Ren L, Li H, et al. Andrographolide alleviates paraquat-induced acute lung injury by activating the Nrf2/HO-1 pathway. Iran J Basic Med Sci (2023) 26 (6): 653-661.

[33] Dandona R, Gunnell D. Pesticide surveillance and deaths by suicide. Lancet Glob Health (2021) 9 (6): e738-e739.

[34] Kim AM. Suicide rates by occupation in Korea, 1993-2017: the impacts of financial crisis and suicide policy. Psychiatry Res (2021) 298: 113787.

[35] Cha ES, Chang SS, Gunnell D, Eddleston M, Khang YH, Lee WJ. Impact of paraquat regulation on suicide in South Korea. Int J Epidemiol (2016) 45 (2): 470-479.

[36] Jamshidi F, Fathi G, Davoodzadeh H. Investigation Paraquat Poisoning in Southwest of Iran- from Sign to Mortality and Morbidity. Arch Med Sadowej Kryminol (2017) 67 (1): 35-45.

[37] Burgos RA, Alarcón P, Quiroga J, Manosalva C, Hancke J. Andrographolide, an Anti-Inflammatory Multitarget Drug: All Roads Lead to Cellular Metabolism. Molecules (2020) 26 (1): 5.

[38] Zhao G, Cao K, Xu C, Sun A, Lu W, Zheng Y, Li H, et al. Crosstalk between Mitochondrial Fission and Oxidative Stress in Paraquat-Induced Apoptosis in Mouse Alveolar Type II Cells. Int J Biol Sci (2017) 13 (7): 888-900.

[39] Rashidipour M, Rasoulian B, Maleki A, Davari B, Pajouhi N, Mohammadi E. Pectin/chitosan/tripolyphosphate encapsulation protects the rat lung from fibrosis and apoptosis induced by paraquat inhalation. Pestic Biochem Physiol (2021) 178: 104919.

[40] Cory S, Adams JM. The Bcl2 family: regulators of the cellular life-or-death switch. Nat Rev Cancer (2002) 2 (9): 647-656.

[41] Endo H, Owada S, Inagaki Y, Shida Y, Tatemichi M. Metabolic reprogramming sustains cancer cell survival following extracellular matrix detachment. Redox Biol (2020) 36: 101643.

[42] Xu H, Shen J, Xiao J, Chen F, Wang M. Neuroprotective effect of cajaninstilbene acid against cerebral ischemia and reperfusion damages by activating AMPK/Nrf2 pathway. J Adv Res (2021) 34: 199-210.

[43] Ryoo IG, Kwak MK. Regulatory crosstalk between the oxidative stress-related transcription factor Nfe2l2/Nrf2 and mitochondria. Toxicol Appl Pharmacol (2018) 359: 24-33.

[44] Tonelli C, Chio IIC, Tuveson DA. Transcriptional Regulation by Nrf2. Antioxid Redox Signal (2018) 29 (17): 1727-1745.

[45] Ahmad MH, Fatima M, Ali M, Rizvi MA, Mondal AC. Naringenin alleviates paraquat-induced dopaminergic neuronal loss in SH-SY5Y cells and a rat model of Parkinson's disease. Neuropharmacology (2021) 201: 108831.

[46] Sies H. Oxidative stress: a concept in redox biology and medicine. Redox Biol (2015) 4: 180-183.

[47] Toygar M, Aydin I, Agilli M, Aydin FN, Oztosun M, Gul H, Macit E, et al. The relation between oxidative stress, inflammation, and neopterin in the paraquat-induced lung toxicity. Hum Exp Toxicol (2015) 34 (2): 198-204.

[48] Pourgholamhossein F, Rasooli R, Pournamdari M, Pourgholi L, Samareh-Fekri M, Ghazi-Khansari M, Iranpour M, et al. Pirfenidone protects against paraquat-induced lung injury and fibrosis in mice by modulation of inflammation, oxidative stress, and gene expression. Food Chem Toxicol (2018) 112: 39-46.

[49] Lv H, Liu Q, Wen Z, Feng H, Deng X, Ci X. Xanthohumol ameliorates lipopolysaccharide (LPS)-induced acute lung injury via induction of AMPK/GSK3β-Nrf2 signal axis. Redox Biol (2017) 12: 311-324.

[50] Huang XT, Liu W, Zhou Y, Sun M, Yang HH, Zhang CY, Tang SY. Galectin-1 ameliorates lipopolysaccharide-induced acute lung injury via AMPK-Nrf2 pathway in mice. Free Radic Biol Med (2020) 146: 222-233.

[51] Ju DT, Sivalingam K, Kuo WW, Ho TJ, Chang RL, Chung LC, Day CH, et al. Effect of Vasicinone against Paraquat-Induced MAPK/p53-Mediated Apoptosis via the IGF-1R/PI3K/AKT Pathway in a Parkinson's Disease-Associated SH-SY5Y Cell Model. Nutrients (2019) 11 (7): 1655.

[52] Chung See WZ, Naidu R, Tang KS. Paraquat and Parkinson's disease: The molecular crosstalk of upstream signal transduction pathways leading to apoptosis. Curr Neuropharmacol (2023).

[53] Jiang F, Li S, Jiang Y, Chen Z, Wang T, Liu W. Fluorofenidone attenuates paraquat induced pulmonary fibrosis by regulating the PI3K/Akt/mTOR signaling pathway and autophagy. Mol Med Rep (2021) 23 (6): 405.

[54] Hsueh YJ, Meir YJ, Yeh LK, Wang TK, Huang CC, Lu TT, Cheng CM, et al. Topical Ascorbic Acid Ameliorates Oxidative Stress-Induced Corneal Endothelial Damage via Suppression of Apoptosis and Autophagic Flux Blockage. Cells 2020 9 (4): 943.

[55] Knight T, Luedtke D, Edwards H, Taub JW, Ge Y. A delicate balance - The BCL-2 family and its role in apoptosis, oncogenesis, and cancer therapeutics. Biochem Pharmacol (2019) 162: 250-261.